Article

Evolution of Heterogeneity and Chemical Functionality during the Oxidation of Graphite

Harish V. Kumar [1], Andrew J. Oyer [1], Kevin Y. -S. Huang [2] and Douglas H. Adamson [1,2,*]

[1] Institute of Materials Science Polymer Program, University of Connecticut, Storrs, CT 06269, USA
[2] Department of Chemistry, University of Connecticut, Storrs, CT 06269, USA
*   Correspondence: adamson@uconn.edu

Abstract: A kinetic study of graphite oxidation provided several insights into the mechanism of graphite oxide (GO) synthesis. The oxidation was observed to occur in two distinct stages, with the first stage lasting for 20 to 30 min and including a rapid disruption of the graphene sp^2 network, the introduction of oxygen functional groups, and an increase in the spacing between the sheets. The second stage saw a marked decrease in the rate of change in spacing, a significant increase in the homogeneity of the GO, little to no further disruption of the sp^2 network, and continuing evolution of the oxygen functionality. The study was based on the analysis by Raman spectroscopy, XRD, FTIR, SEM, and TGA of material taken at various times from a modified Hummers oxidation reaction following work up.

Keywords: graphene oxide; oxidation; kinetics; functional graphene

1. Introduction

Brodie first reported the oxidation of graphite to form graphene oxide (GO) over 150 years ago in an attempt to determine the molecular weight of carbon [1] and GO now plays a central role in a significant number of graphite-based studies [2,3]. Despite this, relatively few investigations focus on the graphite oxidation mechanism: most reports focus on applications and processing techniques. With this in mind, we examine the oxidation of graphite by a commonly used modified Hummers method [4,5], focusing on the kinetics of graphite oxidation to GO. Using relevant characterization methods such as XRD, Raman spectroscopy, SEM, TGA, and FTIR, we show how the structure and homogeneity of GO evolve with increasing oxidation time. The oxidation of graphite is commonly used to facilitate exfoliation and impart hydrophilicity to aid in the processing of graphite [6–8]. Oxidation adds various functionalities to the graphene sheets, frequently changing the hybridization of the carbons comprising the sheets from sp^2 to sp^3 while also increasing the inter-sheet spacing. Descriptions of the preparation and characterization of GO in the literature are often brief, often with only a passing mention of reaction parameters and characterization results.

Past studies of GO synthesis have primarily examined the final GO structure rather than examining intermediate oxidation stages [2,3,9–11]. A recent example is a study that analyzed the effect of commonly used reagents on the final product and suggested the optimum conditions for GO synthesis [12]. Studies aimed at elucidating the mechanism of oxidation are rare. They include the work of Dimiev et al., who showed that GO synthesis techniques' quenching and purification processes significantly affect GO properties and structure [13]. Other examples include the work Rourke et al. [14] and Guo et al. [15] who described the formation of oxidation debris and its effect on the surface activity of GO sheets. Justh et al. reported the characterization of GO at various steps of oxidation, workup, and reduction, observing the changing structure of GO with each step [16]. Investigations specifically considering reaction time are more rare and have focused on narrowly defined

properties. This includes the work of Jeong et al., where the energy gap of GO was tuned by adjusting oxidation time [10], Guo et al., who showed that the morphology and surface topography of hollow GO spheres was affected by the oxidation time of the GO [17], and Shao et al. who used FT-IR to monitor the disappearance of C=C stretching bands [4].

A recently published study by Li et al. is one of very few to study the kinetics of graphite oxidation explicitly [18]. In this study, the authors monitor the disappearance of the oxidant $KMnO_4$ with time at various temperatures and sulfuric acid concentrations. The study also uses an optical examination of individual graphite flakes at different reaction times to study the degree of oxidation of the graphite. The authors conclude that the oxidation involves diffusion of active species at a constant rate into the galleries of the graphite, with the rate being diffusion controlled above a particular oxidant concentration. Structural analysis using XRD, TGA, and XPS was presented, but the findings did not draw any conclusions. Other work has shown the effect of reaction time on the stability of GO dispersions [18–20] and the relationship between reaction time and the size of GO sheets [21,22].

In the study reported here, we performed time-resolved investigations of the oxidation process while examining multiple aspects of the GO to determine the effect that oxidation time had on individual graphene sheets and the sample as a whole. We used a commonly employed modified Hummers' method for the graphite oxidation and sampled the reaction at various times to characterize the state of the material as the reaction proceeded. Like most approaches, the modified Hummers' approach involves strong acids and oxidizers, resulting in a final product containing a distribution of lateral sizes, stacking heights, and degrees of oxidation. Our study reports several novel findings, such as a plateauing of the extent of graphite oxidation with increasing time, a continuing evolution of the oxygen functionality without further oxidation of the GO, an increase in the uniformity of individual GO sheets with increased reaction time, and the apparent stabilization of the structure of isolated GO after approximately two hours of oxidation.

2. Materials and Methods

2.1. Sample Preparation

Graphene oxide was synthesized using a modified Hummers' method [7,23]. Two different graphites were used as described in the text: Ashbury Mills, Grade 3243, 50 μm average flake size natural graphite (graphite 1), and MX 15, 15 μm average flake size synthetic graphite (graphite 2). All experiments were done using graphite 1 unless otherwise mentioned. Concentrated sulfuric acid (100 mL) (Fisher Scientific, ACS Plus) and 2 g of sodium nitrate (Acros Organics, 99%+, ACS Reagent) were added to a flask and stirred until dissolved. Graphite (4 g) was then added to the flask and mixed until dispersed. Finally, 12 g (3 weight equivalents) of potassium permanganate (EM Sciences, GR ACS) was added to the reaction mixture and the solution immediately turned black. The potassium permanganate was added slowly to avoid overheating the system, but quickly enough so that the system did not thicken before all of the oxidant was added. At various times, the reaction was sampled by removing approximately 5 mL of the suspension. Each sample was immediately quenched by its addition to 100 mL of de-ionized (DI) water followed by 10 mL of hydrogen peroxide (Acros Organics, 35 wt.%). After the effervescence slowed, hydrochloric acid (~5 mL) (Sigma Aldrich (Darmstadt, Germany), 37% ACS reagent) was added to solubilize residual salts, and the mixture was filtered and washed until a near neutral wash pH was obtained. The GO was then dialyzed against water using a Spectra/Por Dialysis Membrane (50,000 molecular weight cutoff). To avoid fractionation of the samples, no centrifuge step was used.

2.2. Characterization

Field Emission Scanning Electron Microscopy (FESEM) was performed on a JEOL JSM-6445F/Thermo Noran System Six EDXS with an accelerating voltage of 10.0 kV and a 15 mm working distance. Samples were prepared by adhering dried GO powders to carbon

tape on an SEM stub. Samples were then sputter-coated with a palladium/gold mixture using a Polaron Instruments SEM coating unit E5100 for 30 s.

X-ray Diffraction (XRD) was performed using a Bruker D2 Phaser. For each sample, the graphite powder was tightly packed to generate a smooth surface. Raman spectroscopy was done using a Renishaw 2000 Raman Spectrometer, operating at a wavelength of 514.5 nm. Powder samples were placed on a clean glass slide and scanned three times for ten seconds to minimize fluorescence background over a Raman shift of 1000 to 3200 cm^{-1}. Fourier Transform Infrared Spectroscopy (FTIR) samples were prepared by mixing 1 wt.% GO samples with 99 wt.% KBr (Fisher Scientific (Hampton, NH, USA), IR Grade) pellets. Spectra were collected on a Nicolet Magna-IR 560 spectrometer.

Thermal Gravimetric Analysis (TGA) was performed on a TA Instruments TGA Q-500. Samples were placed inside a platinum DSC pan with small holes punched in the lid. The samples were heated in a nitrogen atmosphere at a rate of 10 °C per minute to a final temperature of 600 °C. Elemental Analysis was obtained using an Elementar Vario Micro cube, where oxygen content was calculated by subtraction. Sedimentation studies were performed by visual observation of GO-in-water dispersions. One milligram of each sample of GO was dispersed in 3 mL of DI water and briefly bath sonicated for fifteen minutes.

3. Results and Discussion

Raman spectroscopy allowed us to monitor the disruption of the sp^2 carbon network in the graphite samples as oxidation proceeded. Raman spectroscopy is an important technique for characterizing GO, and comparing the intensity of the D-band, I(D), that corresponds to a disrupted sp^2 network [24], with the G-band, I(G), that corresponds to an intact sp^2 network, indicates the degree of graphene functionalization [25]. As shown in Figure 1A, spectra from different regions of a single GO sample spread on a glass surface shows a broad range of I(D)/I(G) values. The sample shown was taken immediately after adding the oxidant and worked up by standard techniques and named the 0-min oxidation time sample. Within this single sample, some regions appeared to consist mainly of pristine graphite with no observable D-band, while other regions showed a D-band nearly as intense as the G-band, indicating that oxidation occurred quickly in some sheets but very slowly in others.

Previous studies by Dimiev and Tour [25] proposed that the oxidation of graphite flakes starts at the edges and works in, meaning that the oxidation of individual graphene sheets is not immediately uniform. That mechanism would predict that different regions of a GO sheet would give rise to different Raman spectra, but would not necessarily predict that different sheets within the same GO sample would give very different I(D)/I(G) values. Recognizing that within the same batch of GO there is a large variety of material is of critical importance for application studies using GO. This variation in the degree of oxidation as a function of time was investigated by comparing the Raman spectra of samples taken at different reaction times. For each sample, Raman spectra were obtained from multiple regions and averaged. Figure 1B shows the averaged results using aliquots taken from 0 to 4 h. The increase in the intensity of the D peak relative to the G peak with increasing oxidation time would be expected as the oxidation proceeds [5]. However, the increase was observed to level out, reaching a maximum after approximately thirty minutes, suggesting that the disruption of the sp^2 carbon network was largely finished within the first thirty minutes of oxidation.

Additionally, not necessarily expected was the increase in uniformity of the GO with increasing reaction time. A plot of I(D)/I(G) as a function of oxidation time, shown in Figure 1C, shows a steady increase in the formation of defects with time and a concurrent decrease in the variation within each sample. Although it has long been understood that there is a range of oxidation extents within each GO sample [26,27], this is the first time the heterogeneity has been shown to decrease with increased oxidation time.

While the Raman spectra showed a plateauing of oxidation extent after approximately 30 min, FTIR spectra indicated a continued evolution of the functional groups. This

continued for up to 120 min, as shown in Figure 2A. It is important to note that natural flake graphite can contain numerous peaks in the FTIR, as per previous studies [28]. Of those peaks, we concentrated on three: a peak at approximately 1550 cm^{-1} assigned to sp^2 hybridized C=C in-plane vibrations [29], a peak at approximately 1730 cm^{-1} assigned to non-conjugated carboxylic carbonyl stretching [30,31], and a peak at approximately 1620 cm^{-1} assigned to water [32].
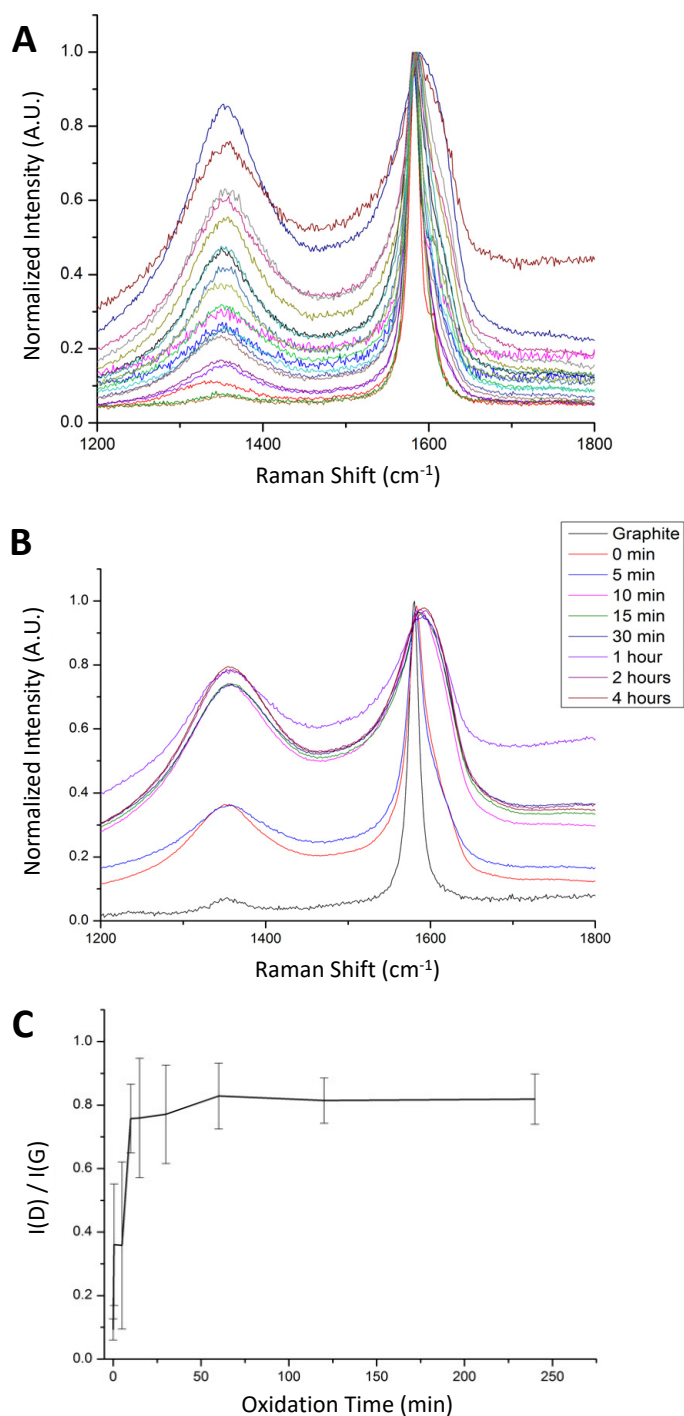

Figure 1. (**A**) Raman spectra of 0 min oxidation time sample at 20 different locations. (**B**) Raman spectra of averaged values at different oxidation times (**C**) I(D)/I(G) ratio as a function of oxidation time. Error bars indicate the difference between maximum and minimum values within each oxidation time.
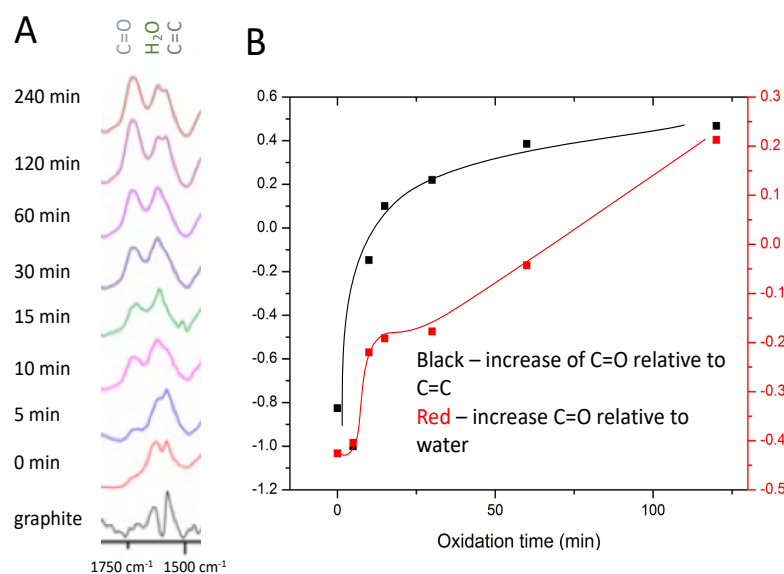
Figure 2. (**A**) FTIR spectra showing the changing relative intensity of the C=C peak at 1550 cm^{-1}, the carboxyl C=O peak at 1730 cm^{-1}, and the peak at 1620 cm^{-1} associated with water. (**B**) Comparison between the carboxyl C=O peak height relative to C=C peak height (black line) and the C=O peak height relative to water (red line) with time by plotting the slope of the line connecting the peak maxima associated with each functional group versus time. The lines are to guide the eye.

The evolution of the three functional groups relative to one another was investigated by plotting the slope of a line between the peak maxima of two peaks versus time to give a relative comparison of the growth (or decline) of the functional groups. The approach employed to generate the plot shown in Figure 2B is described in more detail in Figure S1.

The black line in the plot shown in Figure 2B shows the decline of sp^2 C=C groups at 1550 cm^{-1} relative to the increase in carboxylic carbonyl groups at 1730 cm^{-1} during the reaction. The relative change was initially rapid, slowing after approximately 30 min, reflecting our results from Raman spectroscopy. The water peak at 1620 cm^{-1} in Figure 2A initially appeared as a small shoulder at 0 and 5 min but was fully resolved from 10 min onward, eventually surpassing the height of the carbon-carbon double bond peak. The peak at 1620 cm^{-1} was used as an indication of the amount of water in the GO [33]. Surprisingly, a comparison of the water and the carbonyl peaks, shown by the red line in Figure 2B, showed an increase with time of carbonyl relative to water. This increase occurred in stages, with the rate of increase being fast initially, slowing to near zero from approximately 20 to 30 min, then steadily increasing after 30 min.

The observed decrease in the slope of the red line after approximately 30 min has more than one possible explanation. The first possibility is that both the carbonyl and the water content are increasing with increasing oxidation time. This would mean that the initially fast relative change and leveling off of the red line at approximately 30 min indicates changing relative rates rather than growth of one peak with the other declining. Another possibility is that hydrophilic hydroxyl groups are being replaced with less hydrophilic carbonyl groups, resulting in less water content in the GO as the oxidation proceeds. The positive slope of the black line beyond 30 min would thus be a result of an increase of carbonyl at the expense of hydroxyl groups rather than continued oxidation of the sp^2 network. This would correlate with the Raman spectra plateauing after 30 min, suggesting that while the disruption of the conjugated carbon network by oxidation may be largely finished after 30 min, the type of oxygen functional groups continues to change.

The observed plateau in the overall extent of oxidation was also corroborated by thermogravimetric analysis, TGA, as shown in Figure S2. The precursor graphite does not decompose at temperatures below 600 °C, but significant weight loss occurred for GO samples even after very short oxidation times due to the loss of adsorbed water and

beginning and labile oxygen functional groups. Longer oxidation times further increased the weight loss but with only small increases after 15 min. This observation correlates well with the Raman spectra shown in Figure 1, with little change observed after approximately 30 min. It further suggests, by comparison to FTIR results, that the number of oxygen functional groups in the GO had stabilized after 15 to 30 min, although it is not until approximately 60 min that the TGA curves began to lie on top of one another. Before that, higher temperatures were required to decompose a certain fraction of the GO, a result that might be expected as the decomposition temperature of isolated carboxyl groups would be lower than for conjugated ketones.

Further evidence that the introduction of oxygen functional groups to the sp^2 network had largely stopped after 30 min came from the change in interlayer spacing with time. X-ray diffraction (XRD) was used to determine the spacing present in samples removed at various times, and the results are shown in Figure 3A. The initial graphite sample showed a sharp peak located at a 2θ value of 26.8°, corresponding to a distance between adjacent sheets of 3.34 Å. Oxidation quickly led to a change in sheet spacing, with the XRD pattern of the 0 min sample (sample was taken as quickly as possible following the addition of the oxidizer) already showing a broadened peak. The introduction of oxygen groups and sp^3 hybridized carbon caused an increase in sheet spacing and the appearance of a new peak associated with GO [32].
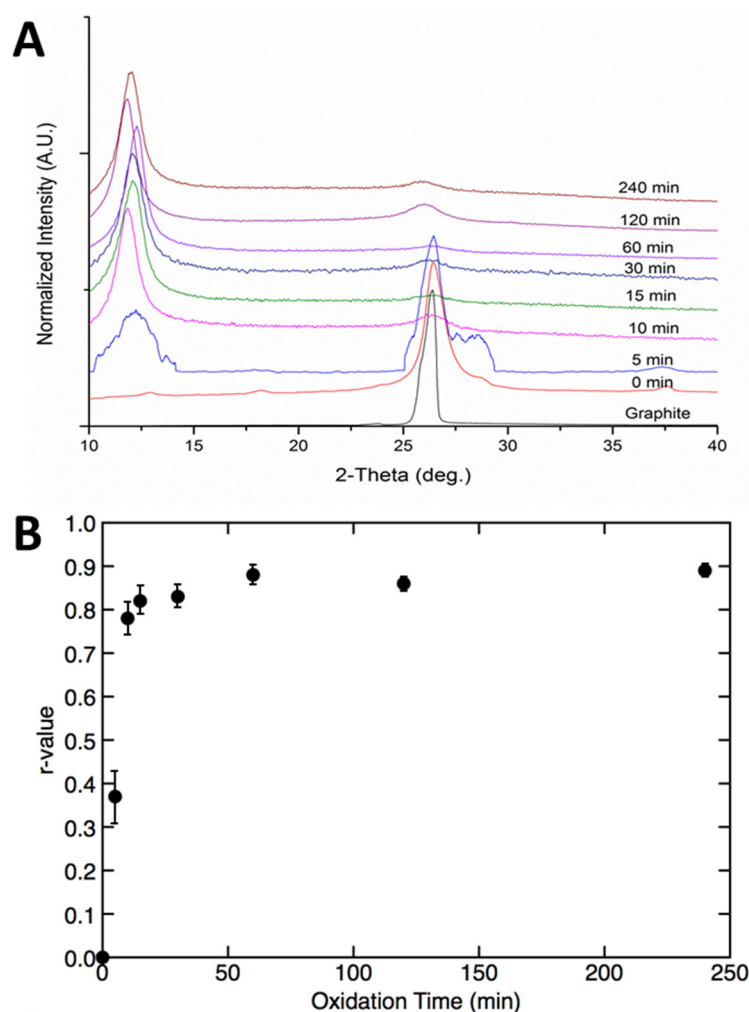

Figure 3. (**A**) X-ray Diffraction of samples from different oxidation times normalized to show peak shift (**B**) r-value indicating growth of GO XRD peak relative to the graphite XRD peak ($A_{GO}/(A_{GO} + A_{G})$) as a function of oxidation time.

The XRD pattern of GO after five minutes of oxidation appeared to be an outlier. A new peak at a lower 2θ value of 10–$13°$, known as the GO peak and corresponding to a d-spacing of 6.5–8 Å, had begun to emerge but was ill-defined and broad. More surprisingly, the peak associated with pristine graphite showed a significant broadening and the appearance of a shoulder. This result was confirmed after repeating the reaction and measurement several times. While the cause of the high 2θ value shoulder was not entirely clear, we suspect it was a result of incomplete diffusion of the oxidizer, causing splaying of the sheet edges at early times. Previous work [26] reported that after adding the first weight equivalent of oxidizer to graphite, a broad curve between 15 and 28° 2θ appeared, indicating the formation of an amorphous phase. While that study analyzed material that was not worked up in aqueous solution, our study analyzed material that had been worked up with conventional aqueous quenching. Thus, while the absolute value of the spacing was expected to be different, the oxidation conditions were comparable. Further oxidation time in our sample resulted in a sharpening of the 10–$13°$ 2θ peak associated with GO, and a steady disappearance of the initial graphite peak. This was also consistent with the findings of the previous study employing their unquenched GO, where additional equivalents of oxidizer sharpened the XRD GO peak.

To quantify the extent of GO formation with time, we compared, within each sample, the XRD peak areas arising from unmodified graphite and oxidized graphite. We plotted the r-value versus oxidation time, where $r = A_{GO}/(A_{GO} + A_G)$, with A_{GO} being the area of the GO peak, and A_G the area of the graphite peak [5]. This plot is shown in Figure 3B and corresponds well with the plot derived from the $I(D)/I(G)$ ratios of the Raman spectra shown in Figure 1C. This plot of oxidation versus time suggests much faster oxidation than expected based on the oxidation times typically reported in the literature.

How this oxidation rate varied with graphite flake size was investigated using the same approach of plotting an r-value vs. time for graphite with different flake sizes. Based on the mechanism of oxidant diffusion, one would expect to find a difference. Figure 4 demonstrates the effect of changing the graphite flake size. Here, graphite 1 (50 μm average size) and graphite 2 (15 μm average size) were used as the starting material in the oxidation. By changing the graphite and keeping other oxidation variables the same, we observed that the smaller flake graphite reached the plateau sooner than the larger flake. Additionally, the smaller graphite flake obtained a significantly higher r-value. The 15 μm graphite oxidized to an r-value of approximately 0.90 within 5 min and reached a value of 0.99 by 20 min. In contrast, the larger 50 μm graphite reached an r-value of only ~0.4 after 5 min, and within 20 min began to plateau near an r-value of 0.8, indicating a greater dispersity of sheet spacing.

SEM images, shown in Figure S3, support the X-ray diffraction data, suggesting that a rapid change in the structure of the graphite occurred during the early oxidation. Untreated graphite appeared to have even and uniform sheet edges, but immediately upon the addition of the oxidizing agent, the basal plane became wrinkled and distorted. The edges of the sheets also appeared less even and contained both bunched and spaced regions. This trend continued through longer oxidation times, producing more uniform basal plane deformations and uncorrelated edges.

A visual analysis of the effect of oxidation time was also informative. One milligram of GO sample, each from different reaction times were sonicated separately in 3 mL of DI water for fifteen minutes. Photographs of these suspensions, taken immediately after sonication and after five days of settling, are shown in Figure S4. As can be seen, the pristine graphite settles, and the resulting 0-min and 5-min samples appear far less dispersed than the others. The degree of GO dispersion increases with oxidation time, suggesting that the hydrophilicity increases with oxidation time. These results also suggest that after approximately 10 min, the rate of graphite modification by oxidation slowed.
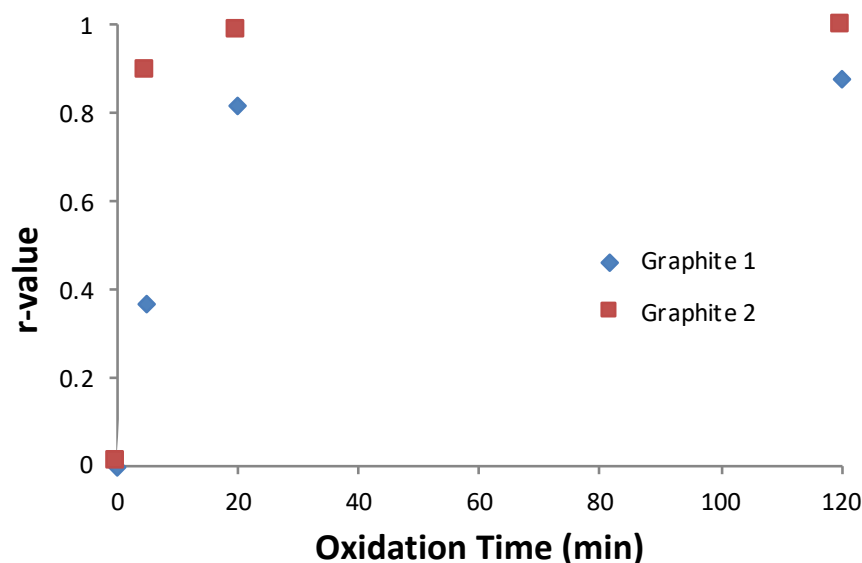
Figure 4. Rate of oxidation of graphite with different starting flake sizes. Graphite 1 was supplied as 50 μm flakes, and graphite 2 was supplied as 15 μm flakes. Time is plotted versus the r-value, derived by comparing the peak areas of each sample at a specific time as obtained by XRD.

4. Conclusions

Our kinetic studies have found both expected and unexpected results. Expected results include the initial decrease in graphite content and increase in GO content with time as observed by XRD, as well as an initial increase in the Raman $I(D)/I(G)$ value with time. Unexpected results include our finding that the GO becomes significantly more homogenous with increasing reaction time, that the oxygen functional groups continue to evolve after 30 min even as the Raman $I(D)/I(G)$ ratio plateaus, and that the oxidation of graphite can be split into two time periods. The material obtained in the first period had oxidized rapidly, as shown with Raman spectroscopy, TGA and XRD, and during the second period, XRD, Raman, and TGA suggest that the rate of oxidation slowed, but FTIR showed a continuing evolution of the oxygen functional groups. Finally, we found that extended oxidation time appeared to create more debris, and this was removed by purification using dialysis in the present work. The remaining GO appeared to remain constant after approximately 60 min. Thus, continued oxidation may consume more graphite while producing more debris, but with little change in the isolated material. Future work will focus on demonstrating the differences that heterogeneity and chemical functionality have on the reactivity and mechanical properties of GO, and the role these aspects play in various applications.

Author Contributions: Conceptualization, A.J.O., H.V.K. and D.H.A.; methodology, A.J.O., H.V.K., K.Y.-S.H. and D.H.A.; investigation, A.J.O., H.V.K. and K.Y.-S.H.; writing—original draft preparation, A.J.O., H.V.K., K.Y.-S.H. and D.H.A.; writing—review and editing, D.H.A.; supervision, D.H.A.; project administration, D.H.A.; funding acquisition, D.H.A. All authors have read and agreed to the published version of the manuscript.

Data Availability Statement: Not applicable.

Conflicts of Interest: The authors declare no conflict of interest. The funders had no role in the design of the study; in the collection, analyses, or interpretation of data; in the writing of the manuscript; or in the decision to publish the results.

References

1. Brodie, B.C. On the Atomic Weight of Graphite. *Philos. Trans. R. Soc. Lond.* **1859**, *149*, 249–259. [CrossRef]
2. Wojtoniszak, M.; Mijowska, E. Controlled oxidation of graphite to graphene oxide with novel oxidants in a bulk scale. *J. Nanoparticle Res.* **2012**, *14*, 1248. [CrossRef] [PubMed]
3. Morimoto, N.; Kubo, T.; Nishina, Y. Tailoring the Oxygen Content of Graphite and Reduced Graphene Oxide for Specific Applications. *Sci. Rep.* **2016**, *6*, 21715. [CrossRef]
4. Shao, G.; Lu, Y.; Wu, F.; Yang, C.; Zeng, F.; Wu, Q. Graphene oxide: The mechanisms of oxidation and exfoliation. *J. Mater. Sci.* **2012**, *47*, 4400–4409. [CrossRef]
5. Kumar, H.V.; Woltornist, S.J.; Adamson, D.H. Fractionation and characterization of graphene oxide by oxidation extent through emulsion stabilization. *Carbon N.Y.* **2016**, *98*, 491–495. [CrossRef]
6. Li, D.; Kaner, R.B. Graphene-Based Materials. *Science* **2008**, *320*, 1170–1171. [CrossRef]
7. Park, S.; Ruoff, R.S. Chemical methods for the production of graphenes. *Nat. Nanotechnol.* **2009**, *4*, 217–224. [CrossRef]
8. Yin, G.; Zheng, Z.; Wang, H.; Du, Q.; Zhang, H. Preparation of graphene oxide coated polystyrene microspheres by Pickering emulsion polymerization. *J. Colloid Interface Sci.* **2013**, *394*, 192–198. [CrossRef]
9. Marcano, D.C.; Kosynkin, D.V.; Berlin, J.M.; Sinitskii, A.; Sun, Z.; Slesarev, A.; Alemany, L.B.; Lu, W.; Tour, J.M. Improved Synthesis of Graphene Oxide. *ACS Nano* **2010**, *4*, 4806–4814. [CrossRef]
10. Jeong, H.K.; Jin, M.H.; So, K.P.; Lim, S.C.; Lee, Y.H. Tailoring the characteristics of graphite oxides by different oxidation times. *J. Phys. D. Appl. Phys.* **2009**, *42*, 65418. [CrossRef]
11. Wang, G.; Yang, J.; Park, J.; Gou, X.; Wang, B.; Liu, H.; Yao, J. Facile Synthesis and Characterization of Graphene Nanosheets. *J. Phys. Chem. C* **2008**, *112*, 8192–8195. [CrossRef]
12. Morimoto, N.; Suzuki, H.; Takeuchi, Y.; Kawaguchi, S.; Kunisu, M.; Bielawski, C.W.; Nishina, Y. Real-Time, in Situ Monitoring of the Oxidation of Graphite: Lessons Learned. *Chem. Mater.* **2017**, *29*, 2150–2156. [CrossRef]
13. Dimiev, A.; Kosynkin, D.V.; Alemany, L.B.; Chaguine, P.; Tour, J.M. Pristine Graphite Oxide. *J. Am. Chem. Soc.* **2012**, *134*, 2815–2822. [CrossRef]
14. Rourke, J.P.; Pandey, P.A.; Moore, J.J.; Bates, M.; Kinloch, I.A.; Young, R.J.; Wilson, N.R. The Real Graphene Oxide Revealed: Stripping the Oxidative Debris from the Graphene-like Sheets. *Angew. Chemie—Int. Ed.* **2011**, *50*, 3173–3177. [CrossRef]
15. Guo, Z.; Wang, S.; Wang, G.; Niu, Z.; Yang, J.; Wu, W. Effect of oxidation debris on spectroscopic and macroscopic properties of graphene oxide. *Carbon N. Y.* **2014**, *76*, 203–211. [CrossRef]
16. Justh, N.; Berke, B.; László, K.; Sziágyi, I.M. Thermal analysis of the improved Hummers' synthesis of graphene oxide. *J. Therm. Anal. Calorim.* **2018**, *131*, 2267–2272. [CrossRef]
17. Guo, P.; Song, H.; Chen, X. Hollow graphene oxide spheres self-assembled by W/O emulsion. *J. Mater. Chem.* **2010**, *20*, 4867–4874. [CrossRef]
18. Li, C.; Shi, Y.; Chen, X.; He, D.; Shen, L.; Bao, N. Controlled synthesis of graphite oxide: Formation process, oxidation kinetics, and optimized conditions. *Chem. Eng. Sci.* **2018**, *176*, 319–328. [CrossRef]
19. Shao, J.-J.; Lv, W.; Yang, Q.-H. Self-assembly of graphene oxide at interfaces. *Adv. Mater.* **2014**, *26*, 5586–5612. [CrossRef]
20. Shen, J.; Hu, Y.; Shi, M.; Lu, X.; Qin, C.; Li, C.; Ye, M. Fast and Facile Preparation of Graphene Oxide and Reduced Graphene Oxide Nanoplatelets. *Chem. Mater.* **2009**, *21*, 3514–3520. [CrossRef]
21. Huang, N.M.; Lim, H.N.; Chia, C.H.; Yarmo, M.A.; Muhamad, M.R. Simple room-temperature preparation of high-yield large-area graphene oxide. *Int. J. Nanomed.* **2011**, *6*, 3443–3448. [CrossRef] [PubMed]
22. Zhang, L.; Liang, J.; Huang, Y.; Ma, Y.; Wang, Y.; Chen, Y. Size-controlled synthesis of graphene oxide sheets on a large scale using chemical exfoliation. *Carbon N. Y.* **2009**, *47*, 3365–3368. [CrossRef]
23. William, S.; Hummers, J.; Offeman, R.E. Preparation of Graphitic Oxide. *J. Am. Chem. Soc.* **1958**, *80*, 1339. [CrossRef]
24. Gómez-Navarro, C.; Meyer, J.C.; Sundaram, R.S.; Chuvilin, A.; Kurasch, S.; Burghard, M.; Kern, K.; Kaiser, U. Atomic Structure of Reduced Graphene Oxide. *Nano Lett.* **2010**, *10*, 1144–1148. [CrossRef]
25. Dimiev, A.M.; Tour, J.M. Mechanism of Graphene Oxide Formation. *ACS Nano* **2014**, *8*, 3060–3068. [CrossRef]
26. Kumar, H.V.; Huang, K.Y.; Ward, S.P.; Adamson, D.H. Altering and investigating the surfactant properties of graphene oxide. *J. Colloid Interface Sci.* **2017**, *493*, 365–370. [CrossRef]
27. Stankovich, S.; Dikin, D.A.; Piner, R.D.; Kohlhaas, K.A.; Kleinhammes, A.; Jia, Y.; Wu, Y.; Nguyen, S.T.; Ruoff, R.S. Synthesis of graphene-based nanosheets via chemical reduction of exfoliated graphite oxide. *Carbon N. Y.* **2007**, *45*, 1558–1565. [CrossRef]
28. Khanra, P.; Lee, C.; Kuila, T.; Kim, H.; Park, J. 7,7,8,8-Tetracyanoquinodimethane-assisted one- step electrochemical exfoliation of graphite and its performance as an electrode material. *Nanoscale* **2014**, *6*, 4864–4873. [CrossRef]
29. Acik, M.; Lee, G.; Mattevi, C.; Chhowalla, M.; Cho, K.; Chabal, Y.J. Unusual infrared-absorption mechanism in thermally reduced graphene oxide. *Nat. Mater.* **2010**, *9*, 840–845. [CrossRef]
30. Trusovas, R.; Raciukaitis, G.; Niaura, G.; Barkauskas, J.; Valucis, G.; Pauliukaite, R. Recent Advances in Laser Utilization in the Chemical Modification of Graphene Oxide and Its Applications. *Adv. Opt. Mater.* **2016**, *4*, 37–65. [CrossRef]

31. Hontoria-Lucas, C.; López-Peinado, A.J.; de López-González, J.D.; Rojas-Cervantes, M.L.; Martín-Aranda, R.M. Study of oxygen-containing groups in a series of graphite oxides: Physical and chemical characterization. *Carbon N. Y.* **1995**, *33*, 1585–1592. [CrossRef]
32. Szabó, T.; Berkesi, O.; Dékány, I. DRIFT study of deuterium-exchanged graphite oxide. *Carbon N. Y.* **2005**, *43*, 3186–3189. [CrossRef]
33. Dimiev, A.M.; Alemany, L.B.; Tour, J.M. Graphene oxide. Origin of acidity, its instability in water, and a new dynamic structural model. *ACS Nano* **2013**, *7*, 576–588. [CrossRef] [PubMed]